

## DISCRETE-TIME PHASE COMPENSATED REPETITIVE CONTROL FOR PIEZOACTUATORS IN SCANNING PROBE MICROSCOPES

Uğur Arıdoğan, Yingfeng Shan and Kam K. Leang\*

Department of Mechanical Engineering  
University of Nevada, Reno  
Reno, Nevada 89557-0312, USA

### ABSTRACT

This paper studies repetitive control (RC) with linear phase lead compensation to precisely track periodic trajectories in piezo-based scanning probe microscopes (SPMs). Quite often, the lateral scanning motion in SPMs during imaging or fabrication is periodic in time. Because of hysteresis and dynamic effects in the piezoactuator, the tracking error repeats from one scanning period to the next. Commercial SPMs typically employ PID feedback controllers to minimize the tracking error; however, the error repeats from one operating cycle to the next. Furthermore, the residual error can be excessively large, especially at high scan rates. A discrete-time repetitive controller was designed, analyzed, and implemented on an experimental SPM. The design of the RC incorporates two phase lead compensators to provide stability and to minimize the steady-state tracking error. Associated with the lead compensators are two parameters that can be adjusted to control the performance of the repetitive controller. Experimental tracking results are presented that compare the performance of PID, standard RC, and the modified RC with phase lead compensation. The results show that the modified RC reduces the steady-state tracking error to less than 2% at 25 Hz scan rate, an over 80% improvement compared to PID control.

### 1 Introduction

Scanning probe microscopes (SPMs), for example atomic force microscopes (AFMs), typically use piezoactuators for positioning the tool tip relative to a sample's surface. These systems commonly operate in a repetitive fashion. For example, in AFM imaging the cantilever probe is scanned across the sample sur-

face by applying a triangle input signal to position the piezoactuator [1] [see Fig. 1]. As the probe moves back and forth over the sample surface, the vertical tip-to-sample interaction is collected and used to construct an image of the sample's topology. Likewise, in nanoindentation an SPM probe is scanned repeatedly in the same fashion and at specific time instances the probe is lowered to create nano-sized indents [2]. During scanning the hysteresis and dynamic effects in the piezoactuator cause significant positioning errors [3] that repeat from one operating cycle to the next. Unfortunately, the error limits the performance of SPMs, such as causing distortion in images and fabricated features. Therefore, precise control of the positioning is needed to obtain high-resolution, undistorted images of the sample [1] and for fabricating uniformly distributed patterns of nano-sized features for the growth of novel structures [2]. In nanofabrication, the size, shape, and spacing of nano features are important to their functionality. This paper specifically addresses the repetitive tracking error in SPM through the design and application of a discrete-time plug-in repetitive control (RC) system. The proposed RC system can be easily integrated into an existing feedback controller in SPMs to handle tracking error associated with periodic motion and/or to reject periodic exogenous disturbances. The RC system consists of two simple phase-lead compensators to ensure stability and minimize the steady-state tracking error. The main contributions of this paper are to analyze the performance of a discrete-time RC system from a practical viewpoint and to describe the important tuning parameters that affect robustness and tracking performance. Also, experimental results are presented to demonstrate the application of RC for AFM.

Repetitive control, a concept based on The Internal Model Principle [4], achieves perfect tracking of periodic trajectories [5, 6]. Compared to traditional proportional-integral (PI) or proportional-integral-derivative (PID) feedback controllers for

\*Corresponding author; Email: kam@unr.edu; Phone/Fax: +1.775.784.7782/1701.

SPM [3], where careful tuning is required and the residual tracking error due to hysteresis and dynamic effects persists from one cycle to the next, a properly designed RC controller will drive the tracking error asymptotically to zero as the number of operating cycles increases [7]. The RC approach achieves precise tracking by incorporating a signal generator within the feedback loop; the signal generator provides infinite gain at the fundamental frequency of the reference trajectory and its harmonics. Such a controller has been investigated to address run-out issues in disk drive systems [7, 8], to generate AC waveforms with low harmonic distortion [9], and to improve the performance of machine tools [10]. However, past work on RC for piezo-based systems and SPMs is limited [11], but it includes a feedback-linearized controller with RC for a piezopositioning stage [12]. This work specifically considers the RC approach for SPM and its implementation in discrete time.

A repetitive controller offers many advantages for SPM applications. For one, it can be plugged into an existing feedback controller to enhance performance for scanning operations. For example, when the piezoactuator scans at a location offset from its center position, the periodic tracking error during scanning can be handled by the repetitive controller and the resident PID controller can be used to account for low frequency dynamics such as creep. But when the reference trajectory is not peri-

odic, the RC controller can be disabled to allow the feedback controller (and/or a feedforward-based controller [1]) to compensate for the tracking error. Compared to iterative learning control (ILC) [13], which is an effective approach that exploits the process of repetition to compensate for hysteresis and dynamic effects in piezoactuators [14, 15], RC does not require the initial condition to be reset at the start of each iteration trial [6]. Resetting the initial conditions adds another level of complexity during implementation. Furthermore, the design and implementation of RC does not require extensive modeling of the system, whereas model-based approaches, such as system inversion [1], require relatively accurate models. It is pointed out that one of the disadvantages with open-loop feedforward control is the lack of robustness when the system dynamics change, for instance under cyclic loading. On the other hand, the feedback mechanism built into RC provides robustness to parameter variation. At the expense of reduced modeling, the RC approach does require accurate knowledge of the period of the reference trajectory. But in SPMs used for imaging and nanofabrication the reference signal's period is often known in advance, and the required period information is far less *a priori* information compared to needing to know the shape of the desired trajectory [1, 15]. Another advantage of RC is it can be easily implemented on a microprocessor due to the lack of complicated algorithms to invert the system model. Therefore, newly available high-speed data acquisition and control hardware can take advantage of the simplicity of RC. This means that RC is attractive for controlling video-rate AFM imaging systems with available digital high-speed hardware [16, 17]. Analog circuit designs have been proposed for implementing RC as well [18].

In the design and application of RC, the major challenges are stability, robustness, and good steady-state tracking performance. The stability and robustness problem has been addressed by incorporating a low-pass filter into the RC loop [19]. Likewise, a simple frequency aliasing filter can be used to stabilize RC and this approach has been applied to a gantry robot [20]. However, a tradeoff is made between robustness and high frequency tracking when such filters are used. The steady-state tracking performance of RC was considered in [21, 22] by cascading a compensator to account for the phase of the low-pass filter. Also, high-order RC was studied in [8] to improve performance and robustness in the presence of noise and variations in period-time. In light of previous work on RC, this paper considers both robust and minimized steady-state error RC design. The majority of previous works considered either one or the other, rarely both. Easy-to-tune linear phase lead compensators are incorporated into the RC design herein. One advantage of the lead compensators is they can be easily implemented in discrete time; therefore, the design can be plugged into existing SPMs to control the positioning of the piezoactuator. The effects of the RC parameters are analyzed and suggestions for how to tune them are provided. Lastly, the proposed RC design was applied to a piezoactuator in a commercial AFM system and experimental results are presented.

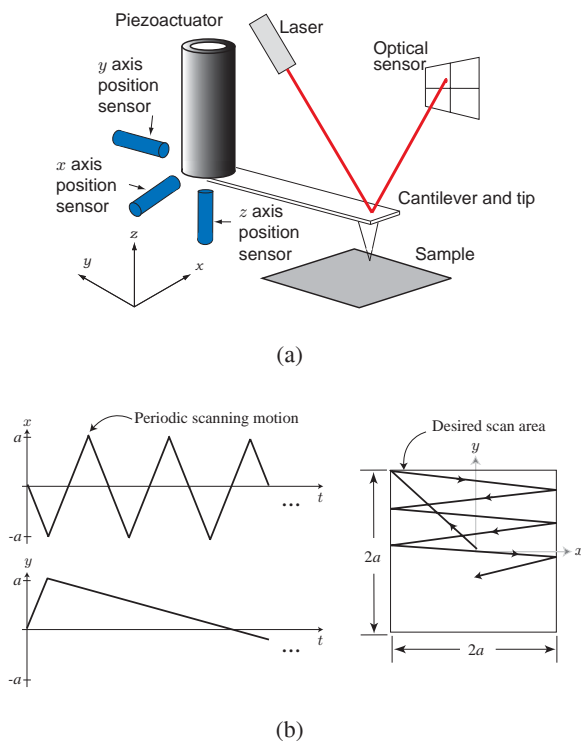


Figure 1. The atomic force microscope (AFM). (a) A schematic of the main components; and (b) a typical scan path in the lateral directions during AFM imaging.

The remainder of this paper is organized as follows. First, Section 2 discusses the RC method and the analysis of the proposed RC design for an example experimental AFM. Section 3 presents the experimental application of RC on AFM tracking and the results are discussed. Finally, Section 5 concludes the paper.

## 2 Repetitive Control Design and Analysis

Repetitive control is a direct application of the Internal Model Principle [4], where perfect tracking of a desired periodic trajectory, with period  $T_p$ , is achieved if the controller consists of the transfer function of the reference trajectory [5, 6, 19]. Such a controller is a signal generator with period  $T_p$ . One advantage of RC is it can be directly inserted into an existing feedback loop as shown in shown in Fig. 2(a).

In the discrete-time closed-loop system in Fig. 2(a), the piezoactuator dynamics are represented by  $G(z)$ , where  $z = e^{j\omega T_s}$ ,  $\omega \in (0, \pi/T_s)$ . The dynamics were assumed to be linear. In the block diagram,  $G_c(z)$  is a feedback controller, such as a resident or otherwise added PID controller in the SPM;  $Q(z)$  is a low-pass filter for robustness;  $k_{rc}$  is the RC gain; and  $P_1(z) = z^{m_1}$  and  $P_2(z) = z^{m_2}$ , where  $m_1, m_2$  are non-negative integers, are positive phase-lead compensators to enhance the performance of the RC feedback system. Particularly, the phase lead compensators  $z^{m_1}$  and  $z^{m_2}$  provide a linear phase lead (in units of radians) of

$$\theta_{1,2}(\omega) = m_{1,2}T_s\omega, \quad \omega \in (0, \pi/T_s). \quad (1)$$

To create a signal generator with period  $T_p$ , the repetitive controller in the inner loop contains the pure delay  $z^{-N}$ , where the positive integer  $N = T_p/T_s$  is the number of points per period  $T_p$  and  $T_s$  is the sampling time. Consider the following assumptions:

**Assumption 1.** The reference trajectory  $R(z)$  is periodic and has period  $T_p$ .

**Assumption 2.** The closed-loop system without the RC loop is asymptotically stable, *i.e.*,  $1 + G_c(z)G(z) = 0$  has no roots outside of the unit circle in the  $z$ -plane.

**Remark 1.** Assumptions 1 and 2 are easily met for SPMs. For example, during imaging the lateral movements of the piezoactuator in SPM are periodic, such as a triangle signal. Also, most SPMs are equipped with feedback controllers  $G_c(z)$  to control the lateral positioning, which can be tuned to be stable.

The transfer function of the signal generator (or RC block) that relates  $E(z)$  to  $A(z)$  is given by

$$\frac{A(z)}{E(z)} = \frac{Q(z)P_1(z)z^{-N}}{1 - Q(z)P_1(z)z^{-N}} = \frac{Q(z)z^{(-N+m_1)}}{1 - Q(z)z^{(-N+m_1)}}. \quad (2)$$

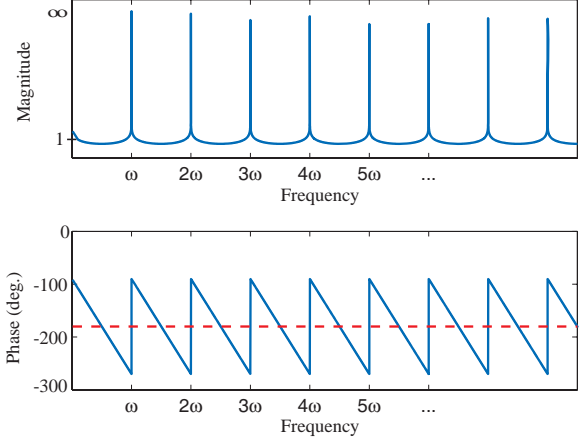


Figure 3. Magnitude and phase versus frequency for signal generator  $z^{-N}/(1 - z^{-N})$ , where  $z = e^{j\omega T_s}$ .

In the absence of the low-pass filter  $Q(z)$  and positive phase lead  $P_1(z) = z^{m_1}$ , the poles of the signal generator are  $1 - z^{-N} = 0$ , hence the frequency response of the signal generator shown in Fig. 3 reveals infinite gain at the fundamental frequency and its harmonics  $\omega = 2n\pi/T_p$ , where  $n = 1, 2, 3, \dots$ . The infinite gain at the harmonics is what gives the RC its ability to track a periodic reference trajectory. As a result, RC is a useful control method for SPM in which the operation is repetitive such as the lateral scanning motion for AFM imaging. Unfortunately, the RC also contributes phase lag which causes instability. Therefore, the stability, robustness, and tracking performance of RC must be considered. It is shown below how the RC gain  $k_{rc}$  and the phase lead compensators  $P_1(z)$  and  $P_2(z)$  affect the RC system's performance. How these parameters should be chosen will also be discussed.

### 2.1 Stability of RC System

Consider the transfer function relating the reference trajectory  $R(z)$  and the tracking error  $E(z)$ ,

$$\frac{E(z)}{R(z)} = \frac{1 - H(z)}{1 - H(z) + [(k_{rc}P_2(z) - 1)H(z) + 1]G_o(z)}, \quad (3)$$

where  $H(z) = Q(z)z^{(-N+m_1)}$  and  $G_o(z) = G_c(z)G(z)$ . Multiplying the numerator and denominator of (3) by the sensitivity function of the feedback system without the repetitive controller,  $S(z) = 1/(1 + G_o(z))$ , the sensitivity function of the closed-loop RC system is given by

$$S_{rc}(z) = \frac{E(z)}{R(z)} = \frac{[1 - H(z)]S(z)}{1 - H(z)[1 - k_{rc}P_2(z)G_o(z)S(z)]}. \quad (4)$$

The stability conditions for the RC system can be determined by simplifying the block diagram in Fig. 2(a) to the equivalent interconnected system shown in Fig. 2(b), which results in

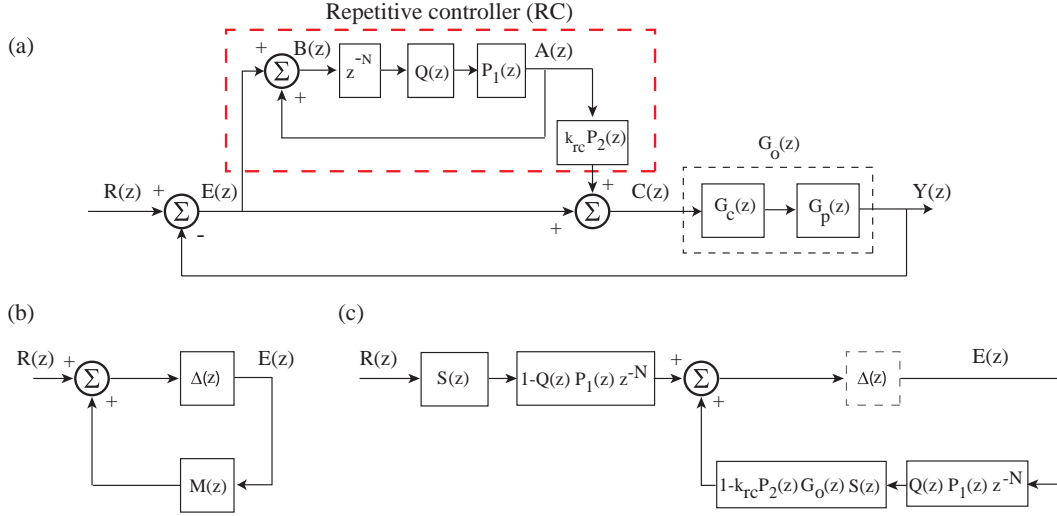


Figure 2. (a) Block diagram of the repetitive control (RC) feedback system. (b) Positive feedback system for stability analysis. (c) Positive feedback system representing the block diagram in part (a) for stability analysis.

Fig. 2(c). Then the RC sensitivity transfer function (4) can be associated with the  $M(z)$  and  $\Delta(z)$  terms in Fig. 2(c) for stability analysis.

**Assumption 3.**  $1 - H(z)$  is bounded input, bounded output stable.

By Assumption 2,  $S(z)$  has no poles outside the unit circle in the  $z$ -plane, so it is stable. Likewise by Assumption 3,  $1 - H(z)$  is stable. Replacing  $z = e^{j\omega T_s}$ , the positive feedback closed-loop system Fig. 2(c) is internally stable according to The Small Gain Theorem [23] when

$$\left| H(z) [1 - k_{rc}P_2(z)G_o(z)S(z)] \right| = \left| H(e^{j\omega T_s}) [1 - k_{rc}e^{j\theta_2(\omega)}G_o(e^{j\omega T_s})S(e^{j\omega T_s})] \right| < 1, \quad (5)$$

for all  $\omega \in (0, \frac{\pi}{T_s})$ , where the phase lead  $\theta_2(\omega)$  is defined by Eq. (1). By satisfying condition (5), the closed-loop RC system shown in Fig. 2(a) is asymptotically stable.

In general, both the RC gain  $k_{rc}$  and the phase lead  $\theta_2(\omega)$  affect the stability and robustness of RC as well as the rate of convergence of the tracking error. Next, condition (5) is used to determine explicitly the range of acceptable  $k_{rc}$  for a given  $Q(z)$  and  $G_o(z)$ . Also, how the phase lead  $\theta_2(\omega)$  affects robustness will be discussed. Afterwards, the effects of the phase lead  $\theta_1(\omega)$  on the tracking performance will be shown. The contributions of these individual parameters on the performance of RC will prove useful during the implementation of RC in Section 3.

## 2.2 The RC Gain and Robustness

Let  $T(z)$  represent the complimentary sensitive function of the closed-loop feedback system without RC, that is,  $T(z) = G_o(z)S(z)$ . Suppose the magnitude of the low-pass filter  $|Q(z)|$

approaches unity at low frequencies and zero at high frequencies, then  $|Q(e^{j\omega T_s})| \leq 1$ , for  $\omega \in (0, \pi/T_s)$ . Next, condition (5) becomes

$$\left| 1 - k_{rc}e^{j\theta_2(\omega)}T(e^{j\omega T_s}) \right| < 1 \leq \frac{1}{|Q(e^{j\omega T_s})|}. \quad (6)$$

Replacing the complimentary sensitive function with  $T(e^{j\omega T_s}) = A(\omega)e^{j\theta_T(\omega)}$ , where  $A(\omega) > 0$  and  $\theta_T(\omega)$  are the magnitude and phase of  $T(e^{j\omega T_s})$ , respectively, Eq. (6) becomes

$$\left| 1 - k_{rc}A(\omega)e^{j[\theta_T(\omega) + \theta_2(\omega)]} \right| < 1. \quad (7)$$

Noting that  $e^{j\theta} = \cos(\theta) + j\sin(\theta)$  and  $k_{rc} > 0$ , Eq. (7) simplifies to

$$-2k_{rc}A(\omega)\cos[\theta_T(\omega) + \theta_2(\omega)] + k_{rc}^2A^2(\omega) < 0, \quad (8)$$

which gives the following two conditions for the RC gain  $k_{rc}$  and linear phase lead  $\theta_2(\omega)$  to ensure stability:

$$0 < k_{rc} < \frac{2\cos[\theta_T(\omega) + \theta_2(\omega)]}{A(\omega)} \quad \text{and} \quad (9)$$

$$-\pi/2 < [\theta_T(\omega) + \theta_2(\omega)] < \pi/2. \quad (10)$$

Condition (10) implies that the lead compensator  $P_2(z) = z^{m_2}$  accounts for the phase lag of the closed-loop feedback system without RC. In fact,  $P_2(z)$  enhances the robustness of the closed-loop RC system by increasing the frequency at which the phase angle crosses the  $\pm 90^\circ$  boundary. This frequency value will be

referred to as the *crossover frequency*. The addition of hysteresis effect and unmodeled dynamics which are not captured by the transfer function  $G_o(z)$  can be taken into account through the lead  $z^{m_2}$ . For example, it has been shown that hysteresis can be treated as phase uncertainty in the open-loop transfer function [24]; hence, the phase lead  $z^{m_2}$  can be adjusted accordingly [22].

### 2.3 Tracking Performance

As previously mentioned, aside from designing RC for stability, it is important to also consider the degree by which the tracking error is reduced relative the tracking error of the original feedback system (without RC). By Assumption 1, where the reference trajectory  $R(z)$  is periodic, the tracking performance of RC can be analyzed by examining the sensitivity function of the RC system at the frequency multiples of the fundamental within the bandpass of the low-pass filter  $Q(z)$ , *i.e.*,  $\omega = k(2\pi/T_p) = k\omega_p$  for  $k = 1, 2, 3, \dots$ .

Recalling Eq. (4), the magnitude of the tracking error at multiples of the fundamental  $\omega_p$  is given by

$$\begin{aligned} |E(e^{jk\omega_p})| &= |S_{rc}(e^{jk\omega_p})R(e^{jk\omega_p})|, \\ &\leq \left| \frac{1-H(e^{jk\omega_p})}{1-H(e^{jk\omega_p})[1-k_{rc}P_2(e^{jk\omega_p})G_o(e^{jk\omega_p})S(e^{jk\omega_p})]} \right| |S(e^{jk\omega_p})| \times \\ &\quad |R(e^{jk\omega_p})|, \\ &\leq |W(e^{jk\omega_p})| \times |S(e^{jk\omega_p})| \times |R(e^{jk\omega_p})|, \end{aligned} \quad (11)$$

where  $W(e^{jk\omega_p})$  is the effect due to the RC. Ideally without the low-pass filter  $Q(z)$ ,  $|W(e^{jk\omega_p})| = 0$  at the multiples of the fundamental frequency  $\omega_p$ . However, the addition of  $Q(z)$  for stability causes phase lag in the RC, which shifts the point of maximum gain of the signal generator created by the pure delay  $z^{-N}$  [12, 21]. Such a shift inadvertently lowers the RC gain at the harmonics and thus negatively effects the tracking performance of the RC system. But much of the phase lag can be accounted for using the linear phase lead  $\theta_1(\omega)$  in the RC loop to improve the tracking performance [22]. Because  $N \gg m_1$ , the modified delay  $z^{-(N+m_1)}$  is causal and can be easily implemented on a microprocessor. Therefore, the value of the phase lead  $\theta_1(\omega)$  can be adjusted through  $m_1$  to minimize the factor  $|W(e^{jk\omega_p})|$  over the frequency range of the bandpass of  $Q(z)$ .

## 3 Implementation of RC for AFM Scanning

The repetitive control scheme in Fig. 2(a) was implemented on an experimental AFM system.

### 3.1 The Experimental AFM System

The experimental AFM system is the Molecular Imaging (MI, now part of Agilent Technologies) PicoPlus model. The AFM uses a piezoelectric tube-shaped actuator for positioning the cantilever and probe tip. The AFM was customized to permit the application of control signals to control the movement of the piezoactuator in the three coordinate axes ( $x$ ,  $y$ , and  $z$ ).

The displacements of the piezoactuator were measured with inductive sensors and the signals were accessible through a custom signal access module. An external computer and data acquisition system running custom C code were used to implement the RC control system. The sampling frequency of the data acquisition and control hardware was 10 kHz.

The RC approach was applied to track a periodic reference trajectory in the  $x$ -axis as an illustrative example. This axis was the fast-scanning axis because the probe tip was moved back and forth at least 100-times faster than the up and down motion in the  $y$ -direction during imaging. For example, a  $100 \times 100$  pixel image requires the AFM tip to scan back and forth across the sample surface 100 times and slowly move from top to bottom [see Fig. 1(b)].

### 3.2 Modeling Piezoactuator Dynamics

A linear dynamics model of the piezoactuator was obtained for designing the RC system. The model was estimated from the measured frequency response function. The frequency response of the piezoactuator along the  $x$  axis was measured using a dynamic signal analyzer (DSA, Hewlett Packard, Model 35670A). The response was measured over small ranges to minimize the effects of hysteresis and above 1 Hz to avoid the effects of creep [1]. The resulting frequency response curves are shown in Fig. 4. A linear  $12^{th}$ -order transfer function model  $G(s)$  (dash-dot line in Fig. 4) was curve fitted to the measured frequency response function. The continuous-time model was then converted to the discrete-time model  $G(z)$  using the Matlab function `c2d` with a sampling frequency of 10 kHz (shown as dash line in Fig. 4).

Commercial SPMs employ traditional PID feedback controllers to minimize hysteresis, creep, and vibrational dynamics. Prior to integrating the RC, a PID controller was designed for the piezoactuator in the  $x$  axis. The PID controller is given by

$$G_c(z) = K_p + K_i \left( \frac{z}{z-1} \right) + K_d \left( \frac{z-1}{z} \right), \quad (12)$$

where the Ziegler-Nichols method was used to tune the controller parameters to  $K_p = 1$ ,  $K_i = 1450$ , and  $K_d = 0.0002$ . The PID controller was implemented with a sampling frequency of 10 kHz. The performance of the PID controller to a step reference is shown in Fig. 5(a). It is interesting to note that without PID control, the open-loop response shows significant overshoot. Also, after 30 ms the drift due to creep becomes noticeable. Creep is a slow behavior and after several minutes the tracking error can be in excess of 20% [14]. On the other hand, the PID controller minimized the overshoot and creep effect.

### 3.3 Closed-Loop PID Control

The response of the PID controller for tracking a triangular trajectory at 1, 5, and 25 Hz are shown in Fig. 5(b). Triangle reference signals are commonly used in AFM imaging. The tracking error versus time for the three cases are shown in Fig. 5(c).

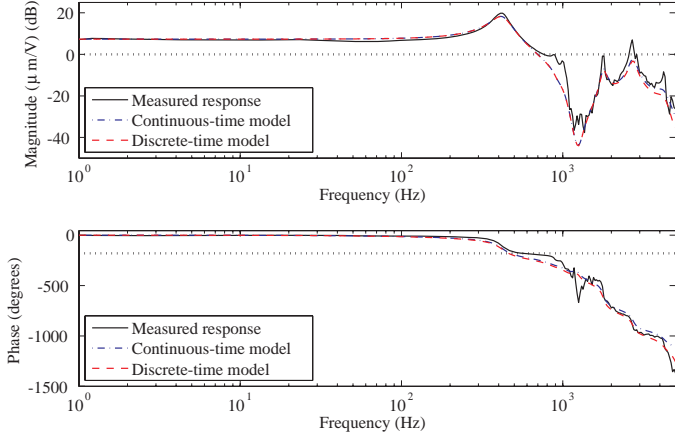


Figure 4. The frequency response of piezoactuator along the  $x$  axis. The solid line is the measured response; the dash-dot line represents the linear continuous-time model  $G(s)$ ; and the dash line is the linear discrete-time model  $G(z)$  using Matlab function `c2d` with zero-order hold and sampling frequency of 10 kHz.

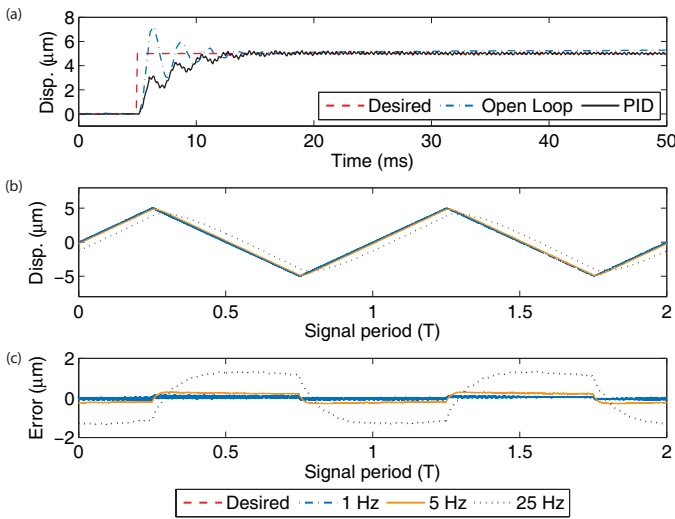


Figure 5. The measured responses of the PID controller for (a) a step reference and (b) triangle references at 1, 5, and 25 Hz. (c) The tracking error for the reference signals associated with plot (b).

The error at 1 Hz (low speed) was relatively small, approximately 1.48% of the 10  $\mu\text{m}$  range ( $\pm 5 \mu\text{m}$ ). However, at 25 Hz (high speed) scanning the error was unacceptably large at 10.70%. Because of vibrational dynamic and hysteresis effects, open-loop AFM imaging is typically limited to less than 2 to 3 Hz. Next, the objective was to further reduce the tracking error by adding a repetitive controller to the PID loop.

### 3.4 Experimental Implementation

Two repetitive controllers were designed, implemented, and their responses were compared to PID control. The first was the standard RC with a low-pass filter  $Q(z)$  in the RC loop and no phase lead compensators. The second RC contained the two

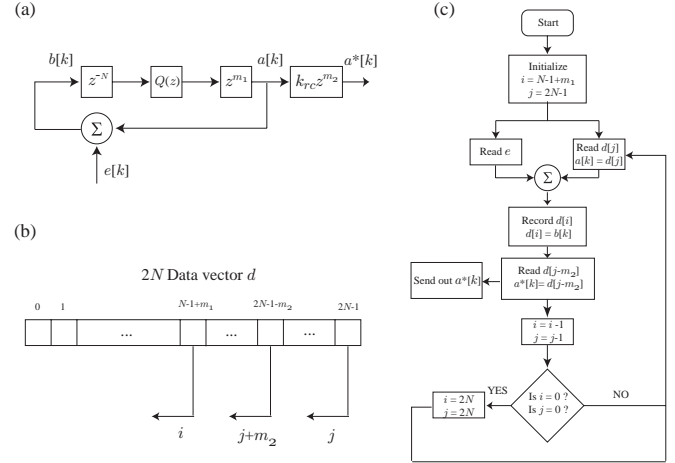


Figure 6. Digital implementation of the RC. (a) Equivalent discrete-time block diagram of the RC loop. (b) Data vector for implementing the one-period delay and the phase lead compensators. (c) The flow diagram for implementing the RC loop.

phase lead compensators  $z^{m_1}$  and  $z^{m_2}$  to control the tracking performance and stability, respectively.

In the experiment, the reference signal was a 25  $\mu\text{m}$  triangle wave at 5, 10, and 25 Hz. The reference trajectory was smoothed using a two-pole, zero-phase-shift filter with cut-off frequency 250 Hz. Triangle scan signals are typically used for AFM imaging and smoothed to avoid exciting high-frequency dynamics. The cutoff frequency for the low-pass filter  $Q(z)$  in the RC loop was 250 Hz. Due to hardware limitations where the sampling frequency was 10 kHz,  $m_2 = 0$  was chosen to give a maximum scan frequency of 25 Hz. The RC gain was chosen as  $k_{rc} = 0.40$  and this value satisfied the condition given by Eq. (9).

The two repetitive controllers were implemented digitally at a sampling frequency of 10 kHz. Let  $N$  be an integer value representing the delay period, the ratio of signal period  $T_p$  to the sampling period  $T_s$ . Figure 6(a) shows the equivalent discrete-time block diagram for the RC loop, where  $z^{-N}$  is a delay of period  $N$ . The two phase lead compensators are shown as  $z^{m_1}$  and  $z^{m_2}$ , where  $m_1 = 6$  and  $m_2 = 0$ . These parameters, in addition to the gain  $k_{rc}$ , were tuned in simulation guided by the conditions (9) and (10) and Eq. (11). Both the delay and phase leads were implemented using a linear data vector  $d$  as shown in Fig. 6(b) with  $2N$  elements. There are two counters  $i$  and  $j$ : one controls the location where incoming data is stored to the data vector and the other controls the location where data is read and sent. The difference in the indices  $i$  and  $j$  determines the overall delay  $-N + m_1 + m_2$ , and since  $N \gg m_1 + m_2$ , then the delay implementation is causal. The flow diagram for the RC implementation with respect to the linear data vector  $d$  is shown in Fig. 6(c). Upon reaching the end of the array at  $i = 0$  and  $j = 0$ , both indices were reset to  $2N - 1$  and the process was repeated.

## 4 Experimental Results and Discussion

The tracking results for the PID, regular RC, and the RC with the phase lead compensators for  $\pm 25 \mu\text{m}$  scanning at 5, 10,

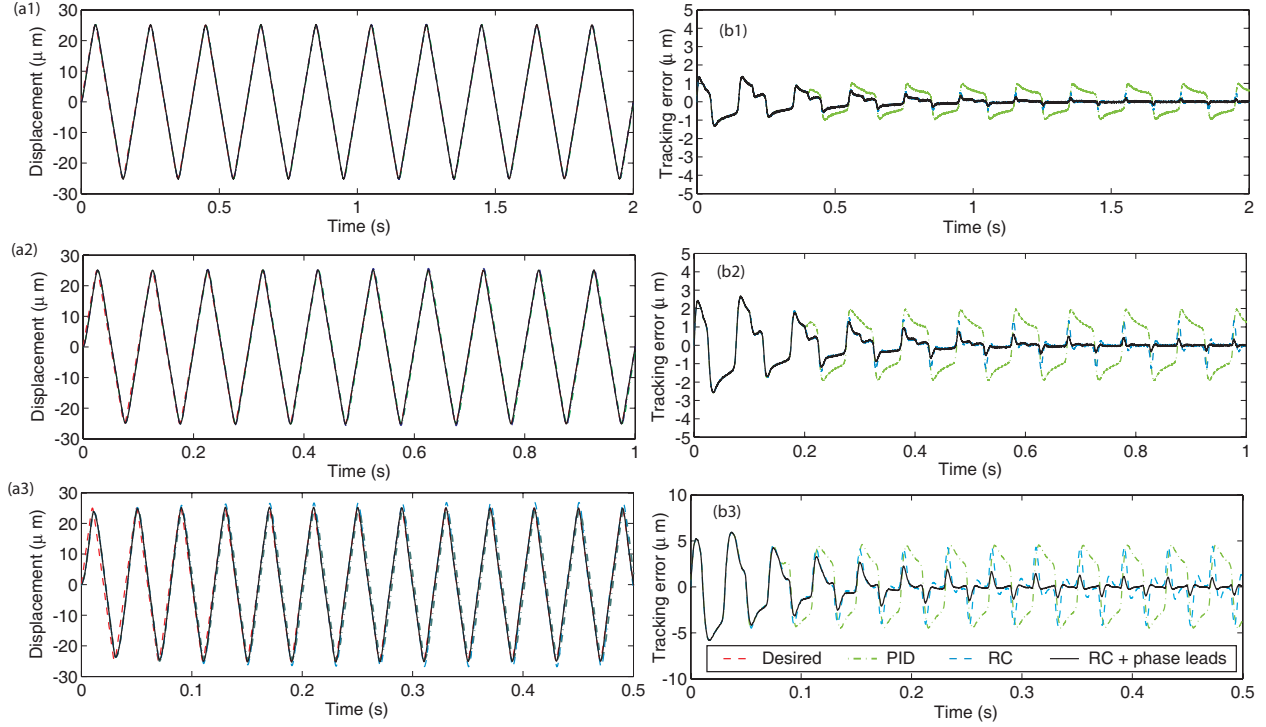


Figure 7. Experimental tracking response and error for PID (dash-dot), RC (dashed line), and RC with phase lead compensation [ $m_1 = 6$  and  $m_2 = 0$ ] (solid line) for 5 Hz (a1 and b1), 10 Hz (a2 and b2), and 25 Hz (a3 and b3) scanning.

Table 1. Tracking results for  $\pm 25 \mu\text{m}$  range. Tracking error reported as percentage of total range.

Controller	5 Hz		10 Hz		25 Hz	
	$e_{max}$	$e_{rms}$	$e_{max}$	$e_{rms}$	$e_{max}$	$e_{rms}$
PID	2.01	1.28	3.99	2.61	9.16	6.61
RC	0.96	0.21	2.74	0.79	8.86	3.69
RC + phase leads	0.43	0.08	0.46	0.10	1.78	0.57

and 25 Hz are presented in Fig. 7 and Table 1. The steady-state tracking errors (last two cycles) are reported as a percentage of the total range; these metrics are described in [14].

Because the action of the repetitive controller is delayed by one scan period, the tracking response for the first period are similar for PID, RC, and RC with phase lead compensation as shown in Fig. 7. However, after the first period the RC begins to work which is evident by the reduction of the tracking error with increasing time. On the other hand, the tracking error of the PID controller persists from one cycle to the next.

The low speed (5 Hz) scanning results shown in Figs. 7(a1) and (b1) and Table 1 demonstrate that the regular RC controller reduced the maximum tracking error from 2.01% to 0.96% compared to the PID controller, a 52% reduction by comparison. By using RC with the phase lead compensation, an additional 55% improvement in tracking performance was achieved. In this case, the maximum tracking error was 0.43%.

At 25 Hz (high speed), the PID tracking error is unacceptable large at 9.16%. In fact, for AFM scanning operations the maximum tracking error should be less than 2%. The results in Table 1 show that the regular plug-in RC controller was also not able to improve the tracking performance at 25 Hz. However, the RC with phase lead compensation gave lower maximum tracking error of 1.78%. Therefore, the RC phase lead compensation enables precision tracking at high speed. The optimum value of the phase lead via  $m_1$  was chosen through trial-and-error method, where  $m_1 = 6$  gave the lowest steady-state tracking error. This value was first determined in simulation, and then validated in the experiment.

Finally, for scanning offset from the piezoactuator's center position, the results are shown in Fig. 8. For this offset scanning operation, the PID controller accounted for the low frequency dynamics such as creep and the RC was used for periodic tracking. The tracking results in Fig. 8 show that the RC was effective at minimizing the tracking error.

## 5 Conclusions

A discrete-time RC controller was designed and analyzed for an experimental AFM system. The RC can easily be combined with the PID feedback system for precision tracking of periodic trajectories. It was shown that one phase lead affects the stability and robustness of the RC closed-loop system; and the other affects the steady-state tracking precision. Experimental results showed that at 25 Hz scan rate, the maximum error was

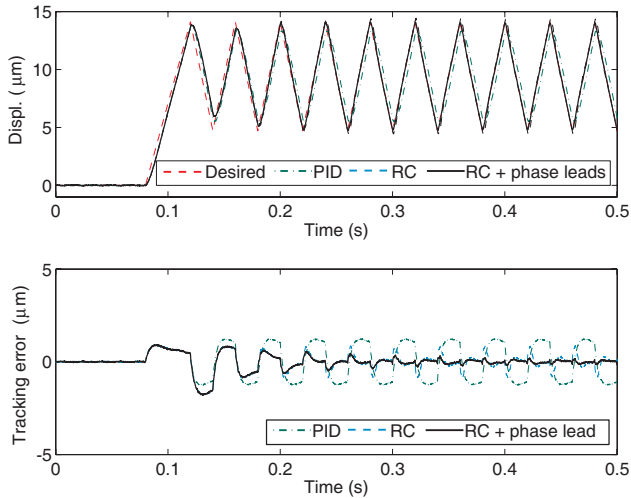


Figure 8. Tracking results for offset triangle scan at 25 Hz. less than 2% using the improved RC technique, where under PID control the error was 9.16%.

## 6 Acknowledgment

This work was supported, in part, by the National Science Foundation Grants DUE #0633098 and CMMI #0726778.

## REFERENCES

[1] D. Croft, G. Shed, and S. Devasia. Creep, hysteresis, and vibration compensation for piezoactuators: atomic force microscopy application. *ASME J. Dyn. Syst., Meas., and Control*, 123:35–43, 2001.

[2] C. Taylor, E. Marega, E. A. Stach, G. Salamo, L. Hussey, M. Munoz, and A. Malshe. Directed self-assembly of quantum structures by nanomechanical stamping using probe tips. *Nanotechnology*, 19:015301, 2008.

[3] R. C. Barrett and C. F. Quate. Optical scan-correction system applied to atomic force microscopy. *Rev. Sci. Instr.*, 62(6):1393–1399, 1991.

[4] B. A. Francis and W. M. Wonham. The internal model principle of control theory. *Automatica*, 12:457 – 465, 1976.

[5] T. Inoue, M. Nakano, and S. Iwai. High accuracy control of a proton synchrotron magnet power supply. In *Proc. 8th World Congr. IFAC*, pages 216 – 221, 1981.

[6] S. Hara, Y. Yamamoto, T. Omata, and M. Nakano. Repetitive control system: a new type of servo system for periodic exogenous signals. *IEEE Trans. Auto. Contr.*, 33(7):659 – 668, 1988.

[7] K. K. Chew and M. Tomizuka. Digital control of repetitive errors in disk drive systems. *IEEE Cont. Syst. Mag.*, pages 16 – 20, 1990.

[8] M. Steinbuch, S. Weiland, and T. Singh. Design of noise and period-time robust high-order repetitive control, with application to optical storage. *Automatica*, pages 2086 – 2095, 2007.

[9] L. Michels, H. Pinheiro, and H. A. Grundling. Design of plug-in repetitive controllers for single-phase PWM invert-

ers. In *IEEE Industry Applications Annual Conference*, pages 163 – 170, 2004.

[10] S.-L. Chen and T.-H. Hsieh. Repetitive control design and implementation for linear motor machine tool. *International Journal of Machine Tools & Manufacture*, 47:1807 – 1816, 2007.

[11] J. Ghosh and B. Paden. Nonlinear repetitive control. *IEEE Trans. Auto. Contr.*, 45(6):949–953, 2000.

[12] G. S. Choi, Y. A. Lim, and G. H. Choi. Tracking position control of piezoelectric actuators for periodic reference inputs. *Mechatronics*, 12(5):669–684, 2002.

[13] K. L. Moore, M. Dahleh, and S. P. Bhattacharyya. Iterative learning control: a survey and new results. *J. Robotic Systems*, 9(5):563–594, 1992.

[14] K. K. Leang and S. Devasia. Design of hysteresis-compensating iterative learning control for piezo positioners: application to atomic force microscopes. *Mechatronics*, 16:141 – 158, 2006.

[15] Y. Wu and Q. Zou. Iterative control approach to compensate for both the hysteresis and the dynamics effects of piezo actuators. *IEEE Control Systems Technology*, 15(5):936 – 944, 2007.

[16] G. Schitter, K. J. Astrom, B. E. DeMartini, P. J. Thurner, K. L. Turner, and P. K. Hansma. Design and modeling of a high-speed AFM-scanner. *IEEE Control Systems Technology*, 15(5):906 – 915, 2007.

[17] K. K. Leang and A. J. Fleming. High-speed serial-kinematic AFM scanner: design and drive considerations. In *American Control Conference*, pages 3188 – 3193, Seattle, WA, USA, 2008.

[18] J. Leyva-Ramos, G. Escobar, P. R. Martinez, and P. Mattavelli. Analog circuits to implement repetitive controllers for tracking and disturbance rejection of periodic signals. *IEEE Transactions on Circuits And SystemsII: Express Briefs*, 52(8):466 – 470, 2005.

[19] M. Tomizuka, T. C. Tsao, and K. K. Chew. Discrete time domain analysis and synthesis of repetitive controllers. In *American Control Conference*, pages 860 – 866, 1988.

[20] J. D. Ratcliffe, P. L. Lewin, and E. Rogers. Stable repetitive control by frequency aliasing. In *Intelligent Control Systems And Optimization*, pages 323 – 326, 2005.

[21] H. L. Broberg and R. G. Molyet. A new approach to phase cancellation in repetitive control. In *IEEE Industry Applications Society Annual Meeting*, volume 3, pages 1766 – 1770, 1994.

[22] Y. Wang, D. Wang, B. Zhang, K. Zhou, and Y. Ye. Robust repetitive control with linear phase lead. In *American Control Conference*, pages 232 – 237, Minneapolis, MN, USA, 2006.

[23] K. Zhou and J. C. Doyle. *Essentials of robust control*. Prentice-Hall, Inc., 1998.

[24] J. M. Cruz-Hernandez and V. Hayward. Phase control approach to hysteresis reduction. *IEEE Trans. Contr. Syst. Tech.*, 9(1):17–26, 2001.